URSI - RCRS 2022, IIT (Indore), India, 1 - 4 December, 2022

Design of Two layer Frequency Selective Rasorber for Dual Band Absorption and In Band Transmission

Alka Dileep* (1), Aditi Sharma (1), Mondeep Saikia(1), Sanjana Paul(1), Dr. Raghvendra Kumar Chaudhary(1), and Dr. Kumar Vaibhav Srivastava(1)
(1) Indian Institute of Technology Kanpur, 208016, email: alkaleep@gmail.com

Abstract

In this paper, a frequency selective rasorber (FSR) with two absorption bands and an in-band transmission window is being proposed. The proposed structure has a two-layer geometry in which the top lossy layer consists of a circular ring having T shaped arm extensions with loaded lumped elements and a circular convoluted loop, whereas the lossless layer consists of an asterisk-based slot. The lossy and lossless layers are separated by an air spacer. The designed unit cell has a periodicity of $0.17\lambda_L \times 0.17\lambda_L$, where λ_L corresponds to the wavelength of the lowest absorption frequency. The equivalent circuit modelling (ECM) concept has been used to design the FSR unit cell. The parametric analysis has been done using the Full wave simulation software. The optimized FSR design exhibits an absorptivity of more than 80% in the frequency ranges of 2.68 GHz to 6.84 GHz and 8.59 GHz to 12.89 GHz. The 3dB transmission bandwidth is in the frequency range of 7.75 GHz to 8.99 GHz with a low insertion loss of 0.29dB at 8.35GHz. The proposed structure can be used for applications that require communication as well as stealth.

1. Introduction

FSS are two dimensional structures or planar periodic arrays that consist of elements repeating in a uniform manner and the geometric specifications as well as the spacing between these elements determine the resonant frequency of these structures. FSS are usually intended to vary the transmission and reflection properties of the electromagnetic waves and can be designed to achieve high pass, low pass, band pass or band stop filter characteristics [1]. Due to these properties FSS can be employed in radome designing, but the out of band signals reflected from these structures will make undesired impact on the RCS reduction. Hence, to overcome such constraints frequency selective rasorbers has been developed and this concept has gained a lot of research interest in the recent times [2]. An FSR combines the functionalities of a radome and an absorber, thereby passing the impinging electromagnetic wave with low insertion loss in the transmission band and absorbing the EM waves otherwise. Based on the position of the absorption (A) and transmission (T) bands, the FSR can be classified into A-T, T-A, A-T-A, T-A-T, A-T-A-T etc. In [3] a T-A type rasorber design comprising of a resistive FSS type top layer and interdigitated Jerusalem cross element-based band pass FSS layer has been proposed. In [4-5] rasorbers with lower band absorption properties and higher band transmission characteristics have been designed. In such absorbers the proximity of the absorption and transmission bands can create strong coupling between the lossy and lossless layer resonators, thus leading to a high insertion loss. Hence, to overcome these issues A-T-A type rasorbers have been proposed [6]. To reduce the number of lumped components used in such designs interdigital resonators have been proposed [7]. An A-T-A FSR based on fractal resonator and double cross FSS layer with a high-Q factor in the transmission band has been proposed for low RCS based radome applications [8]. Further, to satisfy the multiband applications, rasorbers having multiple transmission and absorption bands have been proposed [9].

In this paper an FSR structure with dual band absorption and in-band transmission is designed using two layers. The top lossy layer design having lumped resistors is responsible for the absorption. The bottom layer is a bandpass FSS layer responsible for transmission. In this A-T-A structure the lumped resistor will produce losses thus bringing in absorption and the resonators present in the lossy and lossless layer will together contribute to the transmission. While designing the structure, the aim was to overcome certain limitations such as polarization sensitivity, narrow transmission bandwidth, high insertion loss, wide transition bandwidth, strong out of band signal absorption etc.

2. Design and Analysis of Rasorber

The proposed structure uses a combination of lossy layer loaded with four lumped resistors R=150 Ω and a band pass FSS layer, separated by an air spacer of height t_{air} = 8 mm. As shown in Fig. 1(a), the lossy layer consists of a metallic circular loop attached with four T-shaped arm extensions. Four lumped resistors having 150 Ω resistance each, are imprinted on the T-shaped arms. A circular convoluted loop resonator is integrated within the metallic circular loop. The bandpass FSS layer, as shown in Fig. 1(b), is designed by etching out asterisk slot from the metal coated above the substrate and an asterisk structure with reduced thickness and length is imprinted on that slot. The

mentioned FSS layer design will thus give an asterisk-based slot in the lossless layer. The lossy and lossless layer of the proposed FSR is printed on a 0.79 mm and 0.25 mm thick Rogers 5880 substrate respectively, having a dielectric constant of $\varepsilon_r = 2.2$ and loss tangent (tan δ) equal to 0.0009. The thickness of copper coating is equal to 0.035mm. The isometric view of the proposed FSR is shown in Fig.1(c).

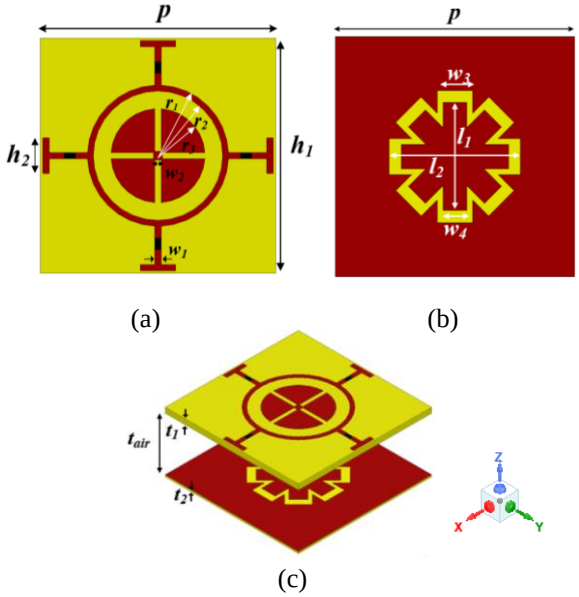

(a) (b)

(c)

Fig. 1. Proposed FSR (a) lossy layer (b) lossless layer (c) isometric view of unit cell geometry. (p = 20, w_1 = 0.55, w_2 = 0.5, h_1 = 18.5, h_2= 3, r_1 =6, r_2 = 5.5, r_3 = 4, w_3 = 3, w_4 = 2, l_1 = 9, l_2 = 11 (units in mm).

The simulated reflection/transmission coefficients of lossy and lossless layers are shown in Fig. 2(a) and Fig. 2(b) respectively. The simulated reflection and transmission coefficients of the proposed FSR are shown in Fig. 2(c). The transmission coefficient curve shows that the 3dB transmission bandwidth is in the frequency range of 7.75 GHz to 8.99 GHz with a low insertion loss of 0.29dB at 8.35GHz. An absorptivity above 80% is observed for two bands from 2.68 GHz to 6.84 GHz and 8.59 GHz to 12.89 GHz as shown in Fig. 2(d).

3. Equivalent Circuit Analysis

The proposed FSR in the above section is designed based on the concept of equivalent circuit modeling discussed in [11] and is shown in Fig. 3. When the electromagnetic wave impinges on the surface of the FSR, a surface current will get generated. The generated surface current will induce capacitive and inductive effects on the gap between the metals and metallic length respectively. Based on this concept, we can model the circuit using distributed elements along with lumped elements if any. The series R-L_1-C_1 combination in the layer 1 is responsible for attaining absorption. The lumped element R, the gap between the adjacent unit cells, and the metallic length of the T-shaped arm contributes to the series R-L_1-C_1 in layer 1.

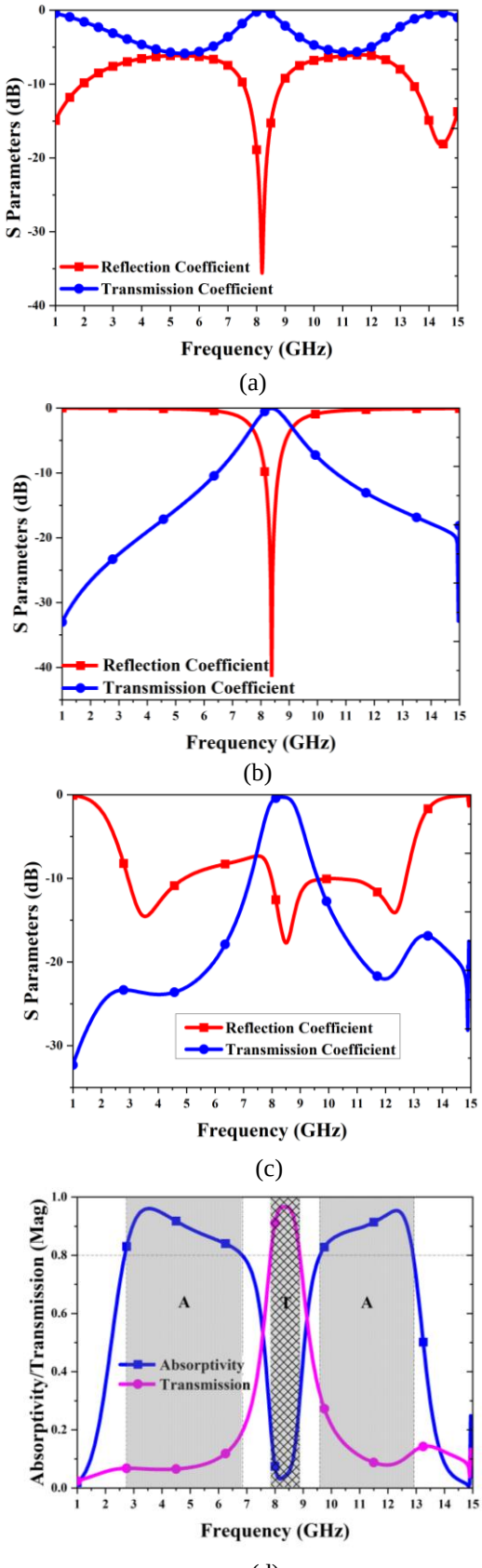

Fig. 2. Simulated parameters (a) lossy layer (b) lossless layer (c) proposed FSR. (d) absorptivity curve of the proposed FSR.

The L_2-C_2 tank circuit in the layer 1 is the simplified equivalent form of the parallel L and C components provided by the circular loop as well as the inner circular convoluted loop resonator. This combination is responsible for the in-band transmission in between the absorption bands produced by the top lossy layer. The equivalent circuit of the bottom FSS layer is modeled using the parallel combination of $L_3 - C_3$, obtained from the metal portion and the slot between the metal portions respectively. The t_{air} is the air spacing between the two layers and is modelled as a transmission line with free space characteristic impedance Z_0 = 377 Ω and thickness equal to 8mm. The top and the bottom dielectric layers (t_1 and t_2 respectively) are represented using a transmission line model with characteristic impedance $Z_d = Z_0/\sqrt{\varepsilon_r}$.While designing an ATA rasorber, it is to be taken care that the transmission frequencies of the lossy and the lossless layers are at least in approximate agreement with each other. This is to ensure that the wave is fully transmitted in those frequencies with the least insertion loss.

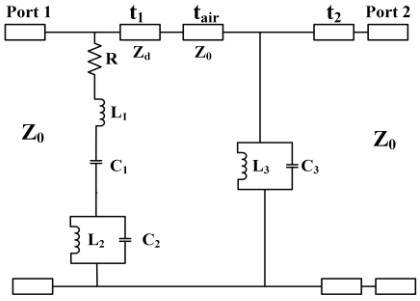

Fig. 3. Equivalent circuit modelling of the proposed FSR. (Circuit parameters are R = 150 Ω, L_1 = 3.763 nH, C_1 = 0.18 pF, L_2 = 0.249 nH, C_2 = 1.516 pF, C_3 = 1.89 pF, L_3 = 0.2 nH, Z_0 = 377 Ω, Z_d = 254.17 Ω, t_1 =0.79 mm

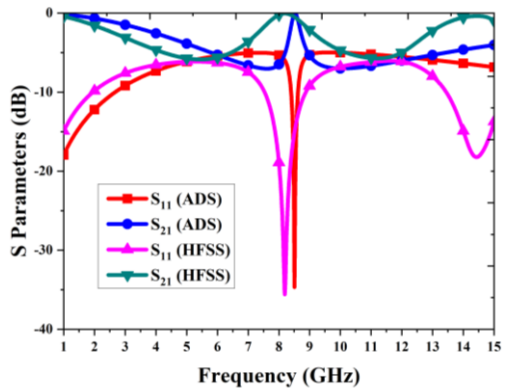

Fig. 4. Comparison of HFSS and ADS simulation of S-Parameter for the proposed FSR.

The comparative plot for the simulated *S*-parameters of the ECM and the HFSS of the proposed FSR is shown in Fig. 4. It can be interpreted from the plots that the trace of the simulated reflection and transmission coefficients of ECM and HFSS follows almost the same pattern.

4. Parametric Analysis

The optimized dimensions for the proposed FSR are obtained after a set of parametric optimizations. The lumped element value R was varied, and it was observed that with the varying R value, the reflection coefficients of the lower and upper band was significantly getting affected as shown in Figure 5. Hence, an optimal value is chosen at R =150 Ω. Similarly, the air-spacer between the two layers has been varied and the corresponding scattering coefficients plots are shown in the Fig. 6. It can be observed that at t_{air} = 8 mm, the rasorber performance is optimum. While designing the unit cell dimensions, it was observed that varying the length and width of the asterisk structure and slot helped to tune the resonant frequency as well as the insertion loss. Similarly varying the h_1 and h_2 values of the T-shaped arm of the lossy layer showed significant impact on the insertion loss.

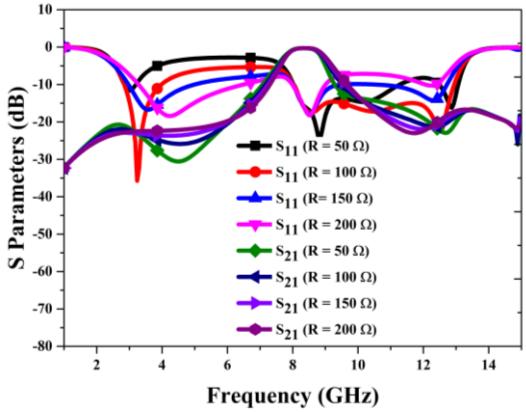

Fig. 5. Simulated reflection and transmission coefficient responses for different values of lumped resistor R.

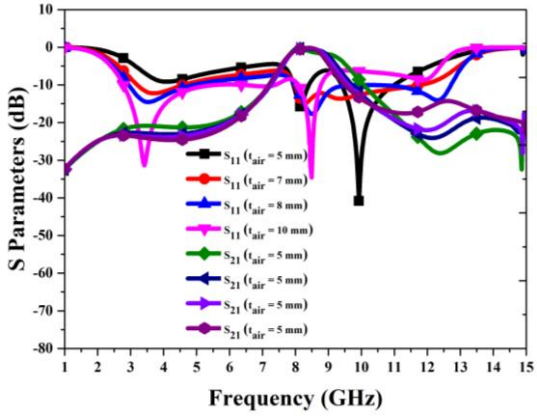

Fig. 6. Simulated reflection and transmission coefficient responses for different values of air gap.

The proposed FSR is further analyzed for different polarization angles of the incident electromagnetic waves and the reflection/transmission coefficient responses are as shown in Fig. 7. It can be observed that the simulated responses remain the same irrespective of the polarization

angles of the incident electromagnetic wave at normal incidence.

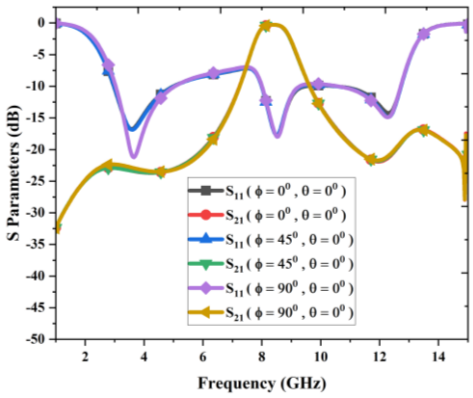

Fig.7. Simulated reflection and transmission coefficient responses for different polarization angles.

The surface current distribution shown in Fig. 8 depicts that during the absorption frequencies, excitation is more prevalent in the circular loops and the T-shaped arms. For the transmission frequency, more current density is observed at the asterisk slot in the bottom layer and the integrated circular convoluted loop in the top layer.

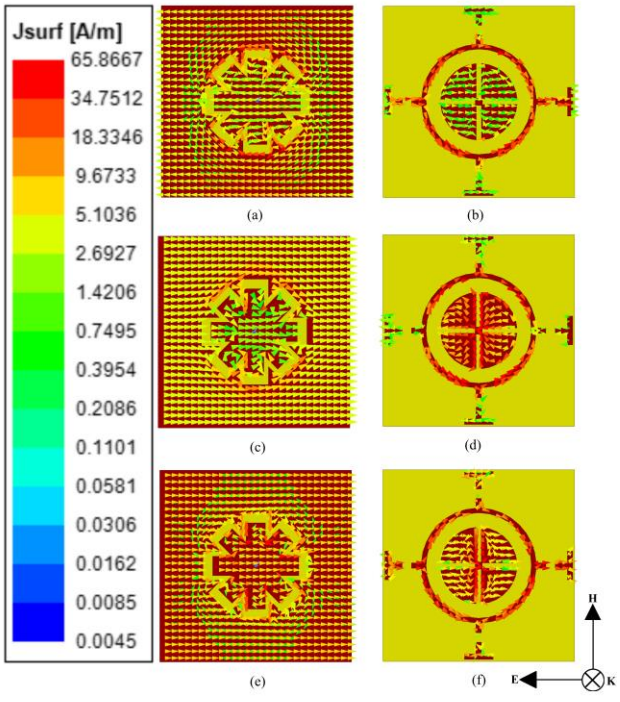

Fig. 8. Surface current distributions on Lossy and lossless layer at different frequencies: (a) 3.52 GHz (b) 3.52 GHz (c) 8.35 GHz (d) 8.35 GHz (e) 12.27 GHz (f) 12.27 GHz.

5. Conclusions

The paper presents a dual- absorption band rasorber with an in-band transmission window. The designed two-layer rasorber exhibited a very low insertion loss at the transmission frequency and two wide band absorptions on either side of the transmission window. The four-fold symmetry of the structure ensures that the design is polarization insensitive. The angular stability of the structure seems to be deteriorating after 15º; hence this is an area that would require further improvement.

6. References

1. B. A. Munk, Metamaterials: Critique and Alternatives. Hoboken, NJ, USA: Wiley, 2009, pp. 62–70.

2. Y. Han, Y. Chang, and W. Che, "Frequency-Selective Rasorbers: A View of Frequency-Selective Rasorbers and Their Application in Reducing the Radar Cross Sections of Antennas," in *IEEE Microwave Magazine*, vol. 23, no. 2, pp. 86-98, Feb. 2022.

3. F. Costa and A. Monorchio, "Absorptive Frequency Selective Radome," in *Proc. URSI General Assem. Scientific Symp*., pp. 1–4, 2011.

4. Q. Chen, L. Chen, J. Bai, and Y. Fu, "Design of Absorptive Frequency Selective Surface with Good Transmission at High Frequency," *Antennas and propagation*, vol. 51, no. 12, pp. 885–886, 2015.

5. Q. Chen, L. Liu, L. Chen, J. Bai, and Y. Fu, "Absorptive Frequency Selective Surface Using Parallel LC Resonance," *Electron. Lett.*, vol. 52, no. 6, pp. 418–419, Mar. 2016.

6.Y. Shang, Z. Shen, and S. Xiao, "Frequency-selective Rasorber Based on Square-Loop and Cross-Dipole Arrays," *IEEE Trans. Antennas Propag*., vol. 62, no. 11, pp. 5581–5589, Nov. 2014.

7. Q. Chen, D. Sang, M. Guo, and Y. Fu, "Frequency-Selective Rasorber with Interabsorption Band Transparent Window and Interdigital Resonator," *IEEE Trans. Antennas Propag*., vol. 66, no. 8, pp. 4105– 4114, Aug. 2018.

8. M. M. Zargar, A. Rajput, K. Saurav and S. K. Koul, "Frequency-Selective Rasorber Based on High-Q Minkowski Fractal-Shaped Resonator for Realizing a Low Radar Cross-Section Radiating System," in *IEEE Transactions on Electromagnetic Compatibility*, 2022.

9. A. Sharma, S. Malik, S. Ghosh and K. V. Srivastava, "A Dual-Transmission Band Rasorber with Miniaturized Unit Cell Geometry," *2021 IEEE International Conference on Electronics, Computing and Communication Technologies (CONECCT)*, 2021, pp. 01-05.

10. Ozdin, Mustafa, Salim Orak, and Faruk Erken. "Design of Broadband Absorptive Optimum Frequency Selective Rasorber without Loaded Circuit Elements," *AEU-International Journal of Electronics and Communications* 127 (2020): 153407.